On the oxygen and nitrogen chemical abundances and the evolution of the "green pea" galaxies

Ricardo O. Amorín
amorin@iaa.es

Enrique Pérez-Montero
epm@iaa.es
and

J. M. Vílchez
jvm@iaa.es
Instituto de Astrofísica de Andalucía (CSIC), Glorieta de la Astronomía S/N, E-18008 Granada, Spain

ABSTRACT

We have investigated the oxygen and nitrogen chemical abundances in extremely compact star-forming galaxies (SFGs) with redshifts between ∼0.11 and 0.35, popularly referred to as "green peas". Direct and strong-line methods sensitive to the N/O ratio applied to their Sloan Digital Sky Survey (SDSS) spectra reveal that these systems are genuine metal-poor galaxies, with mean oxygen abundances ∼ 20% solar. At a given metallicity these galaxies display systematically large N/O ratios compared to normal galaxies, which can explain the strong difference between our metallicities measurements and previous ones. While their N/O ratios follow the relation with stellar mass of local SFGs in the SDSS, we find that the mass–metallicity relation of the "green peas" is offset $\gtrsim$0.3 dex to lower metallicities. We argue that recent interaction-induced inflow of gas, possibly coupled with a selective metal-rich gas loss, driven by supernova winds, may explain our findings and the known galaxy properties, namely high specific star formation rates, extreme compactness, and disturbed optical morphologies. The "green pea" galaxy properties seem to be not common in the nearby universe, suggesting a short and extreme stage of their evolution. Therefore, these galaxies may allow us to study in great detail many processes, such as starburst activity and chemical enrichment, under physical conditions approaching those in galaxies at higher redshifts.

Subject headings: galaxies: dwarf — galaxies: abundances — galaxies: starburst — galaxies: evolution

1. INTRODUCTION

The cosmological relevance of local starbursts is due to their similarities with their analogs at high redshift. They may therefore provide extremely valuable laboratories to study with high resolution and sensitivity relevant physical processes associated with the starburst activity in much better detail. One of the most suitable environments for these purposes can be the intriguing class of very compact, extremely star-forming galaxy (SFG) at low redshift ($0.11 \lesssim z \lesssim 0.35$) recently discovered by volunteers in the "Galaxy Zoo" project (Lintott et al. 2008). These galaxies, popularly referred to as "green peas" (hereafter GPs), were first reported and studied at some length by Cardamone et al. (2009, hereafter C09), who classified more than one hundred of them.

The GPs are rare objects, located in lower-density environments and spectroscopically characterized by very faint continuum emission and strong optical emission lines, namely [OIII]λ5007, with an unusually large equivalent width of up to $\sim$1000Å. These properties along with their extreme compactness (unresolved in Sloan Digital Sky Survey (SDSS) imaging) are the reason for their green colors and point-like appearance in the SDSS plates. According to C09, GPs are low-mass galaxies (stellar masses $M_\star \sim 10^{8.5}$ to $10^{10} M_\odot$) with extremely high star formation rates (SFRs up to 30 $M_\odot$ yr^{-1}), as derived from their emission lines and UV luminosity. Therefore, their specific SFRs (SSFRs, i.e., SFR per unit of mass) are among the highest inferred in the nearby universe. The GP properties are then consistent with the picture of galaxy downsizing (Cowie et al. 1996), where the sites of active star formation shift from high-mass galaxies at early times to lower mass systems at later epoch (see also Bundy et al. 2006; Cowie & Barger 2008; Noeske et al. 2007).

The motivation for this Letter was one of the most striking results obtained by C09: the nearly constant solar metallicity of the GPs (log[O/H]+12$\sim$8.7 in median) over more than two orders of magnitudes in stellar mass. These results would imply strong constrains to the nature of GPs and their evolutionary status. In this Letter we examine in more detail the GP chemical abundances, namely oxygen and nitrogen, and their relation with the stellar mass, using the same SDSS spectra but a different methodology than in C09. This analysis indicates instead, that GPs can be considered as a genuine population of metal-poor galaxies. The results are compared with a larger sample of local SFGs from the SDSS and with a smaller sample of super compact UV-luminous starburst galaxies (Heckman et al. 2005) placed at the same redshift range of the GPs. In particular, the position of GPs in the fundamental relation between mass and metallicity is discussed in the context of their starburst activity and feedback processes.

2. THE DATA

The sample of galaxies was taken from the list of C09. They compiled and analyzed by means of SDSS Data Release 7 (SDSS DR7; York et al. 2000) imaging and spectroscopy, *Hubble Space Telescope (HST)* optical and *GALEX* UV imaging, a well-defined sample of GPs in the redshift range $0.11 \leq z \leq 0.36$ based on color selection criteria. From their list we selected a sub-sample of 79 GPs spectroscopically classified as star-forming systems (their Table 4), ruling out active galactic nuclei (AGNs) according to the diagnostic diagram [N II]/Hα versus [O III]/Hβ (Baldwin et al. 1981). We refer the reader to C09 for a complete description of the sample selection.

We obtained the full set of calibrated one-dimensional spectra, i.e., *spSpec fits* files, from the SDSS archive using the SDSS DR7 query tools[1]. The SDSS spectra cover 3800Å$< \lambda <$9200Å and the fiber has a 3″ diameter which, due to the compactness of the galaxies, include $\gtrsim$70% of the GP $r-$band emission[2]. Emission-line integrated fluxes were consistently measured for each galaxy spectrum using the IRAF task *splot*, by summing all the pixels of the emission line after a linear subtraction of the continuum. The flux uncertainties are then calculated as

$$\sigma_l = \sigma_c \sqrt{N + \frac{EW}{\Delta}} \qquad (1)$$

(Pérez-Montero & Díaz 2003), where σ_l is the line flux uncertainty, σ_c is the uncertainty in the position of the continuum, N is the number of pixels in the flux measurement, EW is the equivalent width of the line and Δ is the wavelength dispersion. In most cases the measurements are in agreement with those based on Gaussian fitting.

3. RESULTS

3.1. Green Peas: A Genuine Population of Metal-poor Galaxies

Physical properties and oxygen and nitrogen ionic abundances were calculated from the measured emission lines using the direct method, which is expected to provide more accurate abundances compared to strong-line methods (see Pérez-Montero & Contini 2009, hereafter

[1] `http://cas.sdss.org/dr7/en/tools/search/sql.asp` and `http://das.sdss.org`

[2] We used $f_{fib} = 10^{-0.4(m_{r,\mathrm{fiber}} - m_{r,\mathrm{Petro}})}$, which is the fraction of the fiber total light (line+continuum) within the fiber aperture

PMC09). First, we have estimated the reddening constant from the Hα/Hβ ratio using the extinction curve of Cardelli et al. (1989). Then, for those objects with a reliable measurement of the [O III] λ 4363 emission line ($\sim$ 70% of the sample), we have derived the [O III] electron temperature. The [O II] electron temperature has been derived from it using the relations proposed by PMC09. O^+, O^{2+}, and N^+ ionic abundances have been calculated using these temperatures and the relative intensities of the corresponding brightest emission lines. Finally, total O/H and N/O abundance ratios have been obtained with the usual expressions (see PMC09).

For the full sample, including those galaxies with no direct determination of the temperature, oxygen total abundances have also been estimated from the strong-line calibrator N2 $\equiv$ log([N II] λ6584/Hα). We have used the empirical relation derived by PMC09, which gives oxygen abundances fully consistent with those derived from T_e-sensitive methods over the whole observed range of metallicity. According to these authors, N2 has a non-negligible dependence on the N/O ratio. Nevertheless, our calculations indicate that correction for this dependence in this sample does not reduce the dispersion, so we have preferred to keep the calculated abundances in the non-corrected form. Regarding N/O, this can be derived using the N2S2 parameter (i.e., [N II]/[S II]), minimizing its dependence on reddening or flux calibration.

We have compared the derived properties of the GPs with two different samples of SFGs. First, we have taken the large sample of emission-line galaxies listed in the Max Planck Institute for Astrophysics/Johns Hopkings University (MPA/JHU) Data catalog of the SDSS DR 7[3], which covers a redshift range $0.03 \leq z \leq 0.37$. We have kept the non-duplicated galaxies with a signal-to-noise ratio (S/N) of at least 5 in all the involved lines. Then, we have discarded those objects classified as AGNs, using the diagnostic diagram [N II]/Hα versus [O III]/Hβ. Finally, we have calculated oxygen and nitrogen abundances in the same way as described above for the sample of GPs. Moreover, using the SDSS SFGs with direct estimation of the ionic abundances, we have obtained the empirical relation between N/O and the N2S2 parameter (PMC09) that was consistently applied to estimate N/O for all the galaxies used in our analysis. Our polynomial fit:

$$\log(\mathrm{N/O}) = -0.76 + 1.94\,\mathrm{N2S2} + 0.55\,(\mathrm{N2S2})^2 \quad (2)$$

where N2S2 = log([N II]/[S II]), gives a slightly higher slope and a much lower dispersion ($\sim$0.1 dex) than the calibration of PMC09.

In addition, we have taken for comparison a sample of 31 nearby ($z < 0.3$) UV-luminous starburst galaxies studied by (Overzier et al. 2008, 2009, 2010). They showed that these galaxies exhibit strong similarities in their properties with the Lyman-break galaxies at high–z, and therefore were proposed as good local Lyman-break analogs (LBAs). Most massive LBAs display a resolved morphology, characterized by the presence of a dominant central object (DCO, Overzier et al. 2009). In contrast, low-mass LBAs are metal-poor galaxies showing close similarities (e.g., morphology, redshift, UV luminosities, size, SSFRs, and environment) to GPs (C09). In fact, three LBAs are also included in the GP sample. These three galaxies are those for which *HST* optical imaging was used to analyze the morphology of the GPs (see Figure 7 in C09). To be consistent, the oxygen

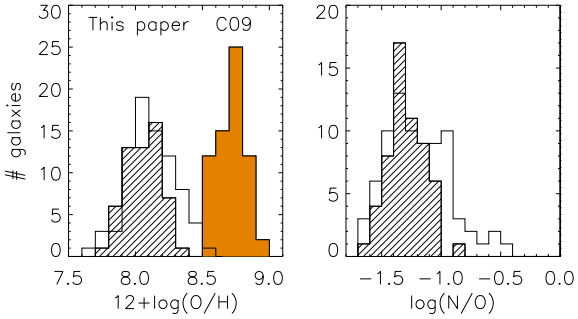

Fig. 1.— Oxygen and nitrogen abundances. On the left, the lined and the non-lined histograms indicate the number of GPs with metallicities calculated from the direct method and using the N2 index, respectively. For comparison, metallicities derived by C09 are shown in the filled histogram. On the right, the lined and the non-lined histograms show the corresponding N/O distributions. (A color version of this figure is available in the online journal.)

[3]Available at http://www.mpa-garching.mpg.de/SDSS/

and nitrogen abundances for the sample of LBAs were re-calculated using the line ratios measured from SDSS spectra (Overzier et al. 2009), and the same empirical calibrations described above.

In Figure 1, we show histograms with our metallicity estimates for the GPs and those derived by C09 for comparison. The GPs show direct metallicities $7.7 \lesssim 12+\log(\mathrm{O/H}) \lesssim 8.4$, with a mean value of 8.05 ± 0.14, i.e., $\sim$20% the solar value[4], whereas their measured C(Hβ) and Hα/Hβ mean values are 0.23 and 3.3, respectively. Our direct estimates and those derived using the N2 parameter agree well in $\sim$0.05 dex. While extinction values are in agreement with those obtained by C09, Figure 1 shows a clear offset of $\sim$0.65 dex between their metallicity estimates (mean $\log(\mathrm{O/H}) + 12 = 8.7$) and ours. The C09 values were obtained using the [N II]λ6584 Å/[O II]$\lambda\lambda$3726, 3729 Å ratio to estimate $\log(\mathrm{O/H}) + 12$ via the theoretical calibration based on photoionization models by Kewley & Dopita (2002). Systematical discrepancies are usually found in the literature between metallicities derived from theoretical and empirical methods (Kewley & Ellison 2008, and references therein). We have used the conversion constants provided by Kewley & Ellison (2008) to scale our N2-based oxygen abundance estimates to those expected from the theoretical calibration (their Table 3). In doing so, we obtained a mean difference of 0.23 dex, which is not enough to explain the largest offset in O/H shown in Figure 1. We conclude that GPs are genuine metal-poor galaxies with low extinction values.

3.2. N/O Ratios and Metallicity

The nitrogen-to-oxygen ratio is a powerful evolutionary indicator in galaxies (Pilyugin et al. 2004; Mollá et al. 2006). We have investigated the relation between the N/O ratio and the oxygen abundance for the sample of GPs, LBAs, and the SFGs taken from the SDSS in Figure 2. For the SFGs, we found a positive trend with an increasing scatter toward the metal-rich regime reflecting both primary and secondary production of nitrogen in the same metallicity range. At low metallicities the trend flattens out, possibly a consequence

[4]We adopted $12+\log(\mathrm{O/H})_\odot = 8.69$ (Allende Prieto et al. 2001)

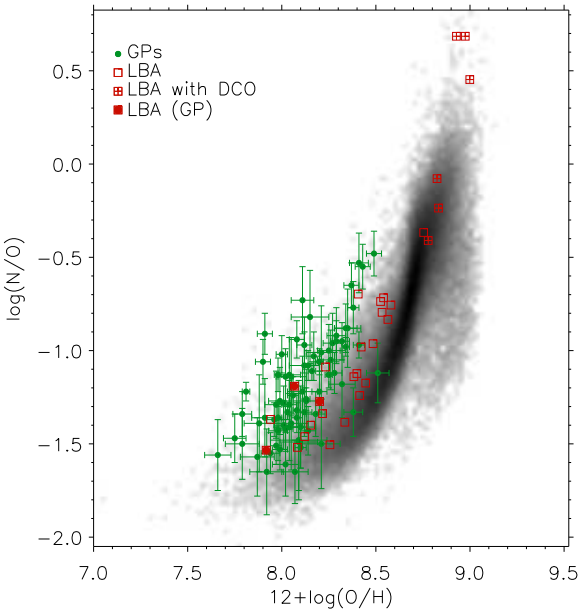

Fig. 2.— N/O vs. O/H. The two-dimensional histogram shows the number distribution of SDSS SFGs in the logarithmic gray scale. GPs are indicated by green circles, while LBAs are indicated with open red squares. LBAs with DCOs are marked with open red squares with plus sign, whereas those LBAs also belonging to the GP sample are indicated with filled red squares. (A color version of this figure is available in the online journal.)

of nitrogen being of primary origin, coming mainly from massive stars. In the low-to-intermediate metallicity range, most GPs and some LBAs display systematically larger N/O ratios for a given metallicity compared to the SDSS SFGs. Possible reasons for this include extra production of primary nitrogen, coming from low-metallicity intermediate-mass stars (Renzini & Voli 1981; Gavilán et al. 2006; Mollá et al. 2006), pollution by Wolf−Rayet stars (e.g., Brinchmann et al. 2008; Lopez-Sanchez & Esteban 2010; Monreal-Ibero et al. 2010), or hydrodynamical effects involving outflow and inflow of gas (van Zee et al. 1998; Köppen & Hensler 2005). This systematically larger N/O ratios could explain the difference between our metallicity and the higher estimates obtained by C09 using the calibration by Kewley & Dopita (2002). The latter assumes that N/O is roughly constant below $12+\log(\mathrm{O/H}) \sim 8.4$, and proportional to O/H

above this value. This implies that larger values of [N II]/[O II] lead to higher metallicities, but this calibration does not take into account the dependence of [N II]/[O II] on the variation of the N/O ratio at a given O/H. According to PMC09, large values of the N/O ratio can enhance the [N II]/[O II] ratio even in the low metallicity regime.

3.3. Relation Between Stellar Mass, Metallicity and the N/O Ratio

In Figure 3, we studied the stellar mass−metallicity relation ($M_\star - Z$, MZR; Lequeux et al. 1979) and the relation between N/O and the stellar mass ($M_\star$−N/O; PMC09) for the GPs, LBAs, and SDSS SFGs. Estimates of $M_\star$ for the three galaxy samples have been taken from C09 (GPs), Overzier et al. (2009, LBAs), and the MPA−JHU catalog (SFGs). They were derived using spectral energy distribution fitting and SDSS photometry. Thus, stellar masses are expected to to be consistent within a typical dispersion of ~ 0.20 dex (e.g., Drory et al. 2004; van der Wel et al. 2006). This value, is lower than the expected uncertainties of 0.3 dex quoted for GPs and LBAs as due to uncertainties in their star formation history (C09; Overzier et al. 2009).

In the $M_\star$−Z plane, SDSS SFGs show a clear positive trend which flattens toward higher masses and show a relatively large scatter at lower masses, in agreement with previous findings for local galaxies (e.g., Tremonti et al. 2004). Similarly, GPs and LBAs increase their metallicity with increasing masses. Nevertheless, GPs lie more than a factor of 2 ($\gtrsim 0.3$ dex) below the MZR of SDSS SFGs, i.e. *at a fixed stellar mass GPs are systematically more metal-poor than normal SFGs.* A similar shift in the MZR has been observed for the less massive ($\log(M_\star) \lesssim 10$) LBAs (Hoopes et al. 2007; Overzier et al. 2010, this work). In terms of stellar mass, the observed offset (as large as 1 dex) largely exceeds the typical uncertainty quoted for the GP masses.

On the other hand, the SDSS SFGs display a correlation between N/O and $M_\star$, with higher N/O ratios at higher stellar masses, in agreement with PMC09 for a different sample of local SFGs. The existence of the $M_\star$−N/O relation reflects the fact that the most massive galaxies evolve more quickly and, hence, they should have on average higher metallicities and N/O ratios. Though the scatter in the $M_\star$−N/O relation is large, most GPs and low-mass LBAs are roughly consistent with the trend of SDSS SFGs, and no systematic offset is observed.

4. DISCUSSION

The shape of the MZR in galaxies has been found to depend on several key processes in galaxy evolution, including the efficiency of star formation (e.g., Lequeux et al. 1979; Mollá & Díaz 2005; Brooks et al. 2007; Calura et al. 2009), the action of metal-rich selective outflows and metal-poor gas inflows (e.g., Larson 1974; Garnett 2002; Tremonti et al. 2004; Finlator & Davé 2008), and the possible variations in the initial mass function (Köppen et al. 2007). Moreover, different amounts of dark matter can also assist in some of these mechanisms (Dekel & Silk 1986).

The GPs follow a relation between mass and metallicity that parallels the MZR defined by the SDSS SFGs, but is offset $\gtrsim$0.3 dex to lower metallicities. Interestingly, we find some remarkable similarities between the GPs and the population of [O III]-selected galaxies of similar luminosity in the z range 0.29–0.42 recently found by Salzer et al. (2009). These galaxies follow a luminosity−metallicity relation that parallels the one defined by SFGs, but is offset by a factor of more than 10 to lower abundances. On the other hand, since GPs and low-mass LBAs lie in a similar offset position in the MZR relative to normal SFGs, their mentioned similarities appear even greater. One possibility to explain their offset position in the MZR is that these galaxies could be still converting a large amount of their cold gas reservoirs into stars. In that case, their low abundances could be due to their relatively young ages compared to normal SFGs. In the same range of masses, both GPs and LBAs have much higher SSFR (typically $>10^{-9}\mathrm{yr}^{-1}$) compared to other SFGs of similar mass (C09). Recent studies show that galaxies with higher SSFRs or larger half-light radii for their stellar mass have systematically lower metallicities (e.g., Tremonti et al. 2004; Ellison et al. 2008). However, we have found even greater under-abundances in the GPs, which have high SSFRs but are extremely compact.

Some models show that in highly concentrated

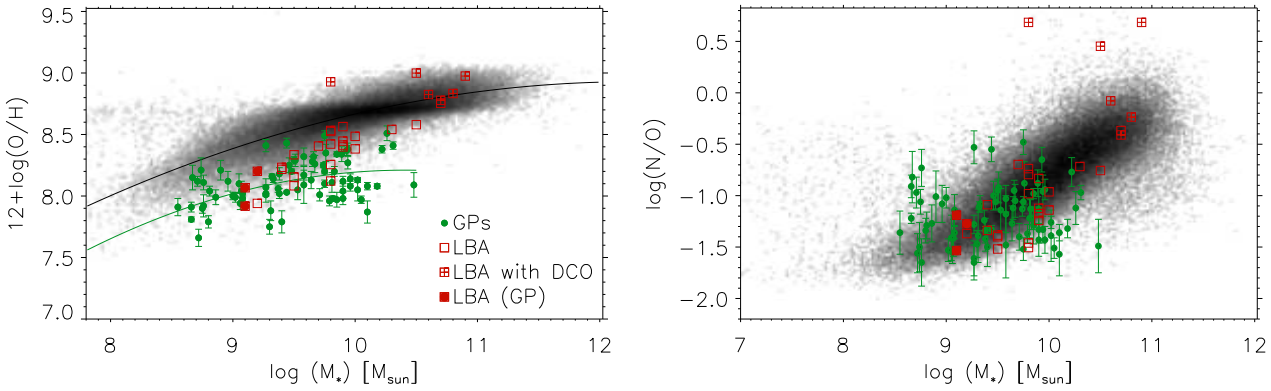

Fig. 3.— $M_\star$ vs. O/H (left) and $M_\star$ vs. N/O (rigth). Symbols stand for the same type of objects as described in Figure 2. For better comparison the trends observed in the $M_\star - Z$ plane, green and black lines indicating second-order polynomial fits to the GPs and SFGs, respectively, have been overplotted. (A color version of this figure is available in the online journal.)

(typical sizes <3 kpc) low-mass galaxies such as the GPs, galactic winds induced by their large SSFR are strong enough to escape from their weak potential wells, diminishing the observed global abundances (e.g., Finlator & Davé 2008). In contrast, analytical models by Dalcanton (2007) show that any subsequent star formation to the outflow will remove their effects on metallicity, unless galaxies have an inefficient star formation. Smoothed particle hydrodynamics (SPH) plus N-body simulations have shown that low star formation efficiencies, regulated by supernova (SN) feedback, could be primarily responsible for the lower metallicities of low-mass galaxies and their overall trend in the MZR (Brooks et al. 2007). As shown by Erb et al. (2006) for SFGs at $z \sim 2$, the constancy in the offset of the MZR suggests the presence of selective metal-rich gas loss driven by SN winds.

Inflow of metal-poor gas, either from the outskirts of the galaxy or beyond, can dilute metals in the galaxy centers, explaining an offset to lower abundances in both the MZR (Mihos & Hernquist 1996; Barnes & Hernquist 1996; Finlator & Davé 2008) and the N/O – O/H diagram. In starburst galaxies, a recent cold gas accretion can be due to interactions, which eventually increases the gas surface density and consequently the star formation. As explained by Ellison et al. (2008), the dilution of metals due to an inflow can be restored by the effects of star formation depending on the dilution-to-dynamical timescale ratio. Since this ratio depends inversely with galaxy radius, galaxies with smaller radius, such as the GPs, may be expected to take longer time to enhance their oxygen abundances to the values expected from the MZR. In this line, the position of GPs in the $M_\star$−N/O relation and the offset observed in the N/O – O/H plane may favor this scenario. Models by Köppen & Hensler (2005) have shown that the rapid decrease of the oxygen abundance during an episode of massive and rapid accretion of metal-poor gas is followed by a slower evolution which leads to the closed-box relation, thus forming a loop in the N/O – O/H diagram.

The inflow hypothesis is also strongly suggested by the disturbed morphologies and close companions observed in spatially resolved *HST* images for three GPs and most LBAs (C09; Overzier et al. 2008). Recent results revealed that galaxies involved in galaxy interactions fall $\gtrsim$0.2 dex below the MZR of normal galaxies due to tidally induced large-scale gas inflow to the galaxies' central regions (e.g., Kewley et al. 2006; Michel-Dansac et al. 2008; Peeples et al. 2009). Several N-body/SPH simulations have shown that major interactions drive starbursts and gas inflow from the outskirts of the H I progenitor disks (e.g., Mihos & Hernquist 1996; Rupke et al. 2010), also supporting this scenario.

We conclude arguing that recent interaction-induced inflow of gas, possibly coupled with a selective metal-rich gas loss driven by SN winds, may

explain our findings and the known galaxy properties. Nevertheless, further work is needed to constrain this possible scenario. In particular, future assessment of the H I gas properties and the star formation efficiency of GPs, as well as the behavior of effective yields with mass compared with models of chemical evolution, will shed new light on the relative importance of the above processes.

Our results allow us to further constrain the evolutionary status of the GPs. These galaxies, as well as the low-mass LBAs and the [O III]-selected galaxies by Salzer et al. (2009) should be analyzed and compared in more detail to elucidate whether these rare objects are sharing similar evolutionary pathways. Even if this is not the case, their properties suggest that these galaxies are snapshots of an extreme and short phase in their evolution. They therefore offer the opportunity of studying in great detail the physical processes involved in the triggering and evolution of massive star formation and the chemical enrichment processes, under physical conditions approaching those in galaxies at higher redshifts.

Forthcoming analysis, based on high S/N intermediate/high-resolution spectroscopy and deep NIR imaging with the Gran Telescopio Canarias (GTC), will be used to better constrain the evolutionary status of the GPs.

We are very grateful to P. Papaderos, M. Mollá and Y. Tsamis for very stimulating discussions and useful suggestions to improve this manuscript. We also thank the anonymous referee for a useful and prompt report. This work has been funded by grants AYA2007-67965-C03-02, and CSD2006-00070: First Science with the GTC (\protecthttp://www.iac.es/consolider-ingenio-gtc/) of the Consolider-Ingenio 2010 Program, by the Spanish MICINN.

Facility: Sloan

REFERENCES

Allende Prieto, C., Lambert, D. L., & Asplund, M. 2001, ApJ, 556, L63

Baldwin, J. A., Phillips, M. M., & Terlevich, R. 1981, PASP, 93, 5

Barnes, J. E., & Hernquist, L. 1996, ApJ, 471, 115

Brinchmann, J., Kunth, D., & Durret, F. 2008, A&A, 485, 657

Brooks, A. M., Governato, F., Booth, C. M., Willman, B., Gardner, J. P., Wadsley, J., Stinson, G., & Quinn, T. 2007, ApJ, 655, L17

Bundy, K., et al. 2006, ApJ, 651, 120

Calura, F., Pipino, A., Chiappini, C., Matteucci, F., & Maiolino, R. 2009, A&A, 504, 373

Cardamone, C., et al. 2009, MNRAS, 399, 1191 [C09]

Cardelli, J. A., Clayton, G. C., & Mathis, J. S. 1989, ApJ, 345, 245

Cowie, L. L., Songaila, A., Hu, E. M., & Cohen, J. G. 1996, AJ, 112, 839

Cowie, L. L., & Barger, A. J. 2008, ApJ, 686, 72

Dalcanton, J. J. 2007, ApJ, 658, 941

Dekel, A., & Silk, J. 1986, ApJ, 303, 39

Drory, N., Bender, R., & Hopp, U. 2004, ApJ, 616, L103

Ellison, S. L., Patton, D. R., Simard, L., & McConnachie, A. W. 2008, ApJ, 672, L107

Erb, D. K., Shapley, A. E., Pettini, M., Steidel, C. C., Reddy, N. A., & Adelberger, K. L. 2006, ApJ, 644, 813

Finlator, K., & Davé, R. 2008, MNRAS, 385, 2181

Garnett, D. R. 2002, ApJ, 581, 1019

Gavilán, M., Mollá, M., & Buell, J. F. 2006, A&A, 450, 509

Heckman, T. M., et al. 2005, ApJ, 619, L35

Hoopes, C. G., et al. 2007, ApJS, 173, 441

Kewley, L. J., & Dopita, M. A. 2002, ApJS, 142, 35

Kewley, L. J., & Ellison, S. L. 2008, ApJ, 681, 1183

Kewley, L. J., Geller, M. J., & Barton, E. J. 2006, AJ, 131, 2004

Köppen, J., & Hensler, G. 2005, A&A, 434, 531

Köppen, J., Weidner, C., & Kroupa, P. 2007, MNRAS, 375, 673

Larson, R. B. 1974, MNRAS, 169, 229

Lequeux, J., Peimbert, M., Rayo, J. F., Serrano, A., & Torres-Peimbert, S. 1979, A&A, 80, 155

Lintott, C. J., et al. 2008, MNRAS, 389, 1179

Lopez-Sanchez, A. R., & Esteban, C. 2010, arXiv:1004.0626

Michel-Dansac, L., Lambas, D. G., Alonso, M. S., & Tissera, P. 2008, MNRAS, 386, L82

Mihos, J. C., & Hernquist, L. 1996, ApJ, 464, 641

Mollá, M., & Díaz, A. I. 2005, MNRAS, 358, 521

Mollá, M., Vílchez, J. M., Gavilán, M., & Díaz, A. I. 2006, MNRAS, 372, 1069

Monreal-Ibero, A., Vilchez, J. M., Walsh, J. R., & Munoz-Tunon, C. 2010, arXiv:1003.5329

Noeske, K. G., et al. 2007, ApJ, 660, L43

Overzier, R. A., et al. 2008, ApJ, 677, 37

Overzier, R. A., et al. 2009, ApJ, 706, 203

Overzier, R. A., Heckman, T. M., Schiminovich, D., Basu-Zych, A., Gonçalves, T., Martin, D. C., & Rich, R. M. 2010, ApJ, 710, 979

Peeples, M. S., Pogge, R. W., & Stanek, K. Z. 2009, ApJ, 695, 259

Pérez-Montero, E., & Díaz, A. I. 2003, MNRAS, 346, 105

Pérez-Montero, E., & Contini, T. 2009, MNRAS, 398, 949 [PMC09]

Pilyugin, L. S., Vílchez, J. M., & Contini, T. 2004, A&A, 425, 849

Renzini, A., & Voli, M. 1981, A&A, 94, 175

Rupke, D. S. N., Kewley, L. J., & Barnes, J. E. 2010, ApJ, 710, L156

Salzer, J. J., Williams, A. L., & Gronwall, C. 2009, ApJ, 695, L67

Tremonti, C. A., et al. 2004, ApJ, 613, 898

van Zee, L., Salzer, J. J., & Haynes, M. P. 1998, ApJ, 497, L1

van der Wel, A., Franx, M., Wuyts, S., van Dokkum, P. G., Huang, J., Rix, H.-W., & Illingworth, G. D. 2006, ApJ, 652, 97

York, D. G., et al. 2000, AJ, 120, 1579

This 2-column preprint was prepared with the AAS LaTeX macros v5.2.